# 1. Supplementary Methods

## 1.1. Sample- and variant-level quality control

Sample- and variant-level quality control was performed using R package SNPRelate v.1.6.4 [1]. For sample-level quality control, patients with >5% missing genotypes, excessive heterozygosity (inbreeding coefficient |F|>0.1), or identity by descent (IBD) kinship coefficient > 0.1 were excluded. For variant-level quality control, genetic variants deviated from Hardy-Weinberg equilibrium (p-value cut-off $<1\times10^{-6}$) within each PCA-based ancestry and/or variants with call rate <95 % were excluded.

## 1.2. Principal component analysis (PCA)

PCA was performed using Eigenstrat [2] with HapMap phase III as a reference (n=861 individuals). Based on the first two eigenvectors, if patients were within 6 standard deviations of defined reference populations, ancestry was assigned as one of three categories: African (AFR), East Asian (EAS), or European (EUR).

## 1.3. Base model development (Step 1 in Figure 1)

The structural base model was built sequentially starting with irinotecan and followed by SN-38, SN-38G, and APC. One-, two-, and three- compartments with linear and nonlinear (Michaelis-Menten) elimination were evaluated to describe the pharmacokinetics of each compound. The structural base model selection was based on goodness-of-fit plots (observed vs. model-predicted plots and conditional and individual weighted residual plots), log-likelihood estimated by Monte Carlo importance sampling method, information criteria including Akaike's information criteria (AIC) [3], Bayesian information criteria (BIC) [4], and precision of parameter estimates.

## 1.4. Covariate analysis of demographic and clinical factors (Step 2 in Figure 1)

As a screening step, potential significant covariates were first explored by examining the relationship between random effects of pharmacokinetic parameters ($\eta_{CL1}$ and $\eta_{CL4}$) and demographic/clinical factors at an α level of 0.05. Demographic/clinical factors with p<0.05 from one-way analysis of variance (ANOVA) for categorical variables or Pearson's correlation test for continuous variables were incorporated into the model by stepwise forward inclusion.

For continuous covariates (age, BSA, and pre-treatment total bilirubin), power and exponential functions normalized by median value were evaluated, as in the following examples:
Power function:

$$CL_i = CL_{pop} \cdot \left(\frac{BSA}{BSA_{median}}\right)^{\beta_{CL}} \cdot e^{\eta_{CL,i}} \quad (1)$$

Exponential function:

$$CL_i = CL_{pop} \cdot e^{\beta_{CL} \cdot \left(\frac{BSA}{BSA_{median}}\right)} \cdot e^{\eta_{CL,i}} \quad (2)$$

where $CL_i$ is the model-predicted clearance of the i[th] individual, $CL_{pop}$ is the population mean value of clearance, $BSA$ is body-surface area of the i[th] individual, $BSA_{median}$ is median body-surface area of the population, $\beta_{CL}$ is the covariate effect of body-surface area on clearance, and $\eta_{CL,i}$ is the normally distributed individual random effect with a mean of 0 and a variance of $\omega^2$.

For categorical covariates (gender, genetically-determined ancestry, and co-administration of irinotecan with 5-fluorouracil/leucovorin and bevacizumab), the exponential function was evaluated as in the following example:

$$CL_i = CL_{pop} \cdot e^{\beta_{CL,sex}} \cdot e^{\eta_{CL,i}} \quad (3)$$

where $CL_i$ is the parameter estimate of clearance of the i[th] individual, $CL_{pop}$ is the population mean value of clearance in male subjects (male=0), $\beta_{CL,sex}$ is the coefficient for influence of gender on clearance in female subjects (female=1), and $\eta_{CL,i}$ is the normally distributed individual random effect with a mean of 0 and a variance of $\omega^2$.

For the stepwise forward inclusion, demographic/clinical covariates were added one at a time and retained in the model if the covariate significantly reduces the -2 log-likelihood (-2LL) by at least 3.84 ($p < 0.05$, $\chi^2$ distribution with 1 degree of freedom).

**1.5. Tree-based model**

A non-parametric regression tree model [5] was developed based on the recursive partitioning methods within a general theory of permutation tests [6]. Briefly, 1) the global null hypothesis of the independence between the target variable and input variables are tested. If this hypothesis is rejected, the algorithm will be stopped. If this hypothesis is not rejected, the input variable with the strongest association with the target variable will be selected. The association is measured by a p-value for the partial null hypothesis of the independence between a single input variable and the target variable. 2) Patients are split into two groups according to the selected input variable. 3) Steps 1) and 2) are repeated.

## 2. Supplementary Figures

**Figure S1. Flow chart of the quality control.** VIP, Very Important Pharmacogenes (www.pharmgkb.org) [7].

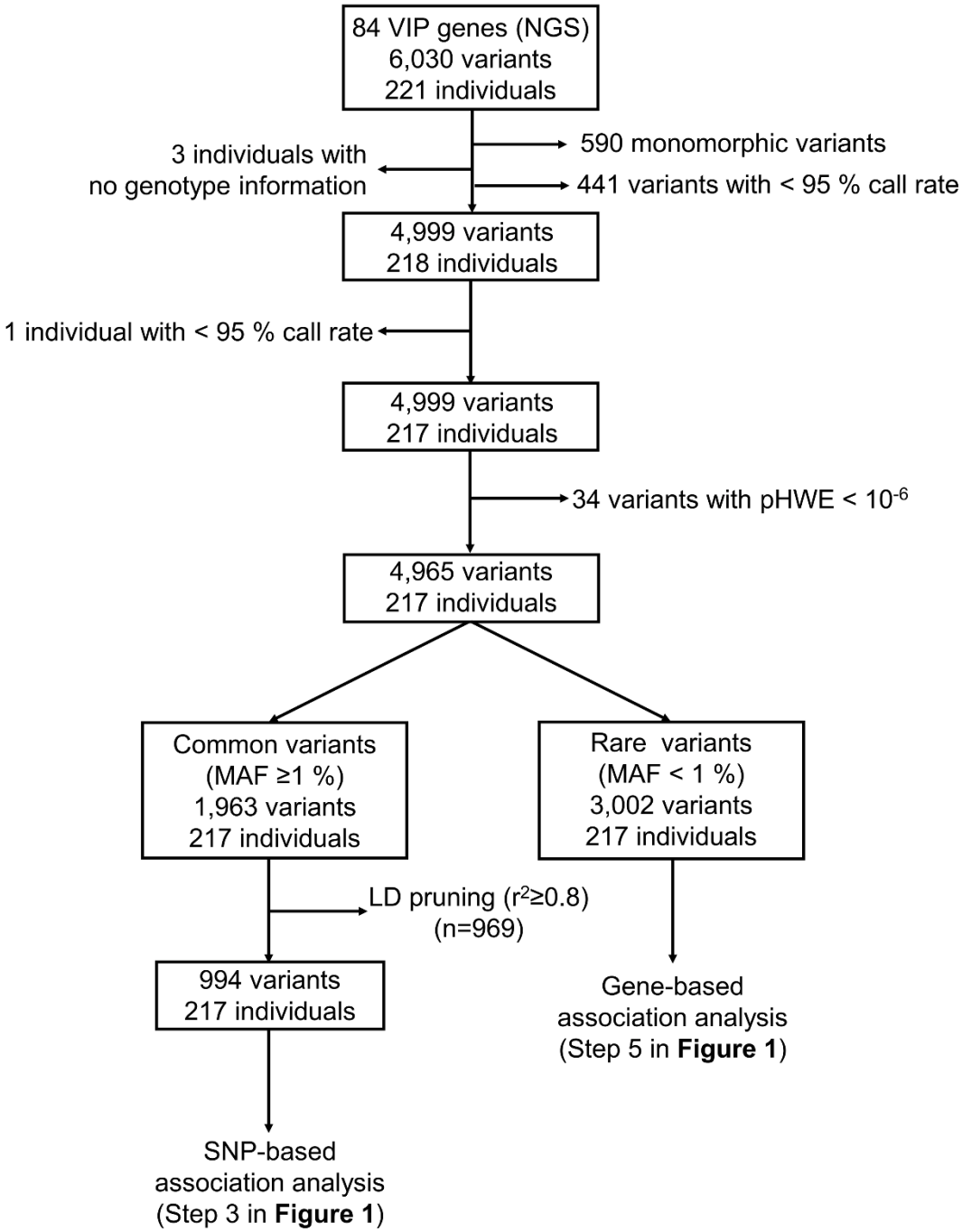

**Figure S2. Structural population pharmacokinetic model of irinotecan (CPT-11), SN-38, SN-38G, and APC (Step 1 in Figure 1).**

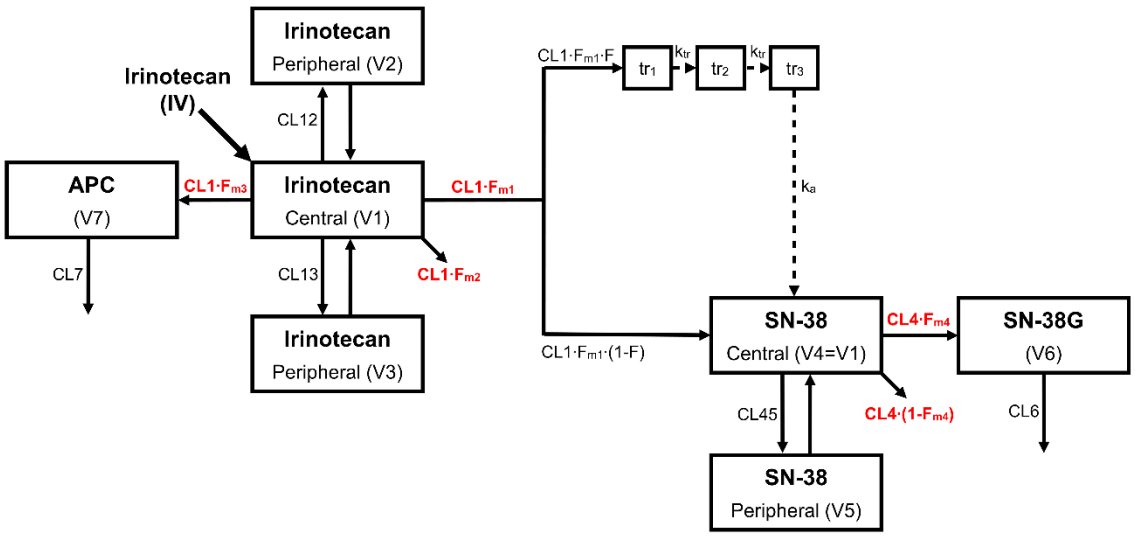


Abbreviations: **CL1**, clearance of irinotecan (CL1=(CL1·$F_{m1}$) + (CL1·$F_{m2}$) + (CL1·$F_{m3}$), where $F_{m1}+F_{m2}+F_{m3}=1$); **CL12**, slow inter-compartmental clearance of irinotecan; **CL13**, fast inter-compartmental clearance of irinotecan; **CL4**, clearance of SN-38 (CL4=(CL4·$F_{m4}$) + (CL4·(1-$F_{m4}$))); **CL45**, inter-compartmental clearance of SN-38; **CL6**, clearance of SN-38G; **CL7**, clearance of APC; **F**, fraction of irinotecan undergoing delayed metabolism to SN-38 through transit compartment process; **$F_{m1}$**, fraction of irinotecan dose metabolized to SN-38; **$F_{m2}$**, fraction of irinotecan dose eliminated through other routes; **$F_{m3}$**, fraction of irinotecan dose metabolized to APC; **$F_{m4}$**, fraction of SN-38 metabolized to SN-38G; **$k_{tr}$**, **$k_a$**, first-order transit rate constants; **$tr_1$**, **$tr_2$**, **$tr_3$**, transit compartments; **V1**, volume of the central compartment of irinotecan; **V2**, volume of the slow-equilibrating peripheral compartment of irinotecan; **V3**, volume of the fast-equilibrating peripheral compartment of irinotecan; **V4**, volume of the central compartment of SN-38; **V5**, volume of the peripheral compartment of SN-38; **V6**, volume of the central compartment of SN-38G; **V7**, volume of the central compartment of APC.

**Supplementary Figure S3. Correlations between irinotecan dose received by patients and clearances of irinotecan and SN-38.** Correlations between (a) irinotecan dose and irinotecan clearance and (b) irinotecan dose and SN-38 clearance were evaluated using all trials (n=217) (**A**), trial 2 only (n=37) (**B**), and after excluding trial 2 (n=180) (**C**). For **A** and **B**, clearance values were obtained from the final model including all trials (**Supplementary Table S3**). For **C**, clearance values were estimated and obtained from the final model after excluding trial 2. Data points represent individual patient data. Solid black and red lines represent best fitted linear and LOESS lines, respectively.

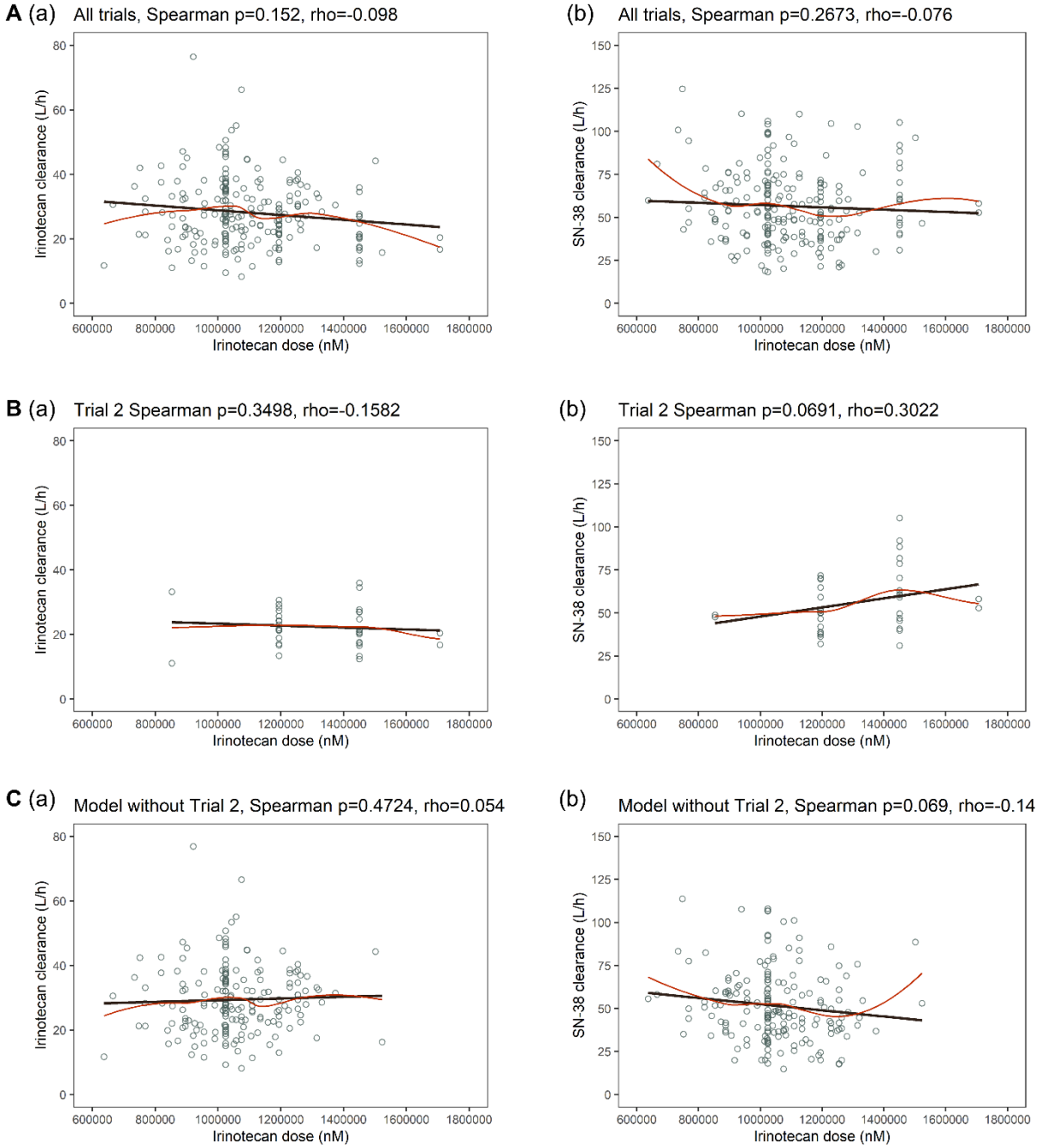

**Figure S4. Goodness-of-fit plots of the final population pharmacokinetic model (Step 8 in Figure 1) of irinotecan (A), SN-38 (B), SN-38G (C), APC (D).** Plots of **(a)** observed vs. individual predicted concentrations (nM), **(b)** observed vs. population predicted concentrations (nM), **(c)** individual weighted residuals (IWRES) vs. time (hour) after administration of irinotecan, **(d)** IWRES vs. predicted concentrations (nM), **(e)** population-weighted residuals (PWRES) vs. time (hour) after administration of irinotecan dose, **(f)** PWRES vs. predicted concentrations (nM). The black and orange lines represent the line of unity and loess fit, respectively. The circles represent data points for each patient.

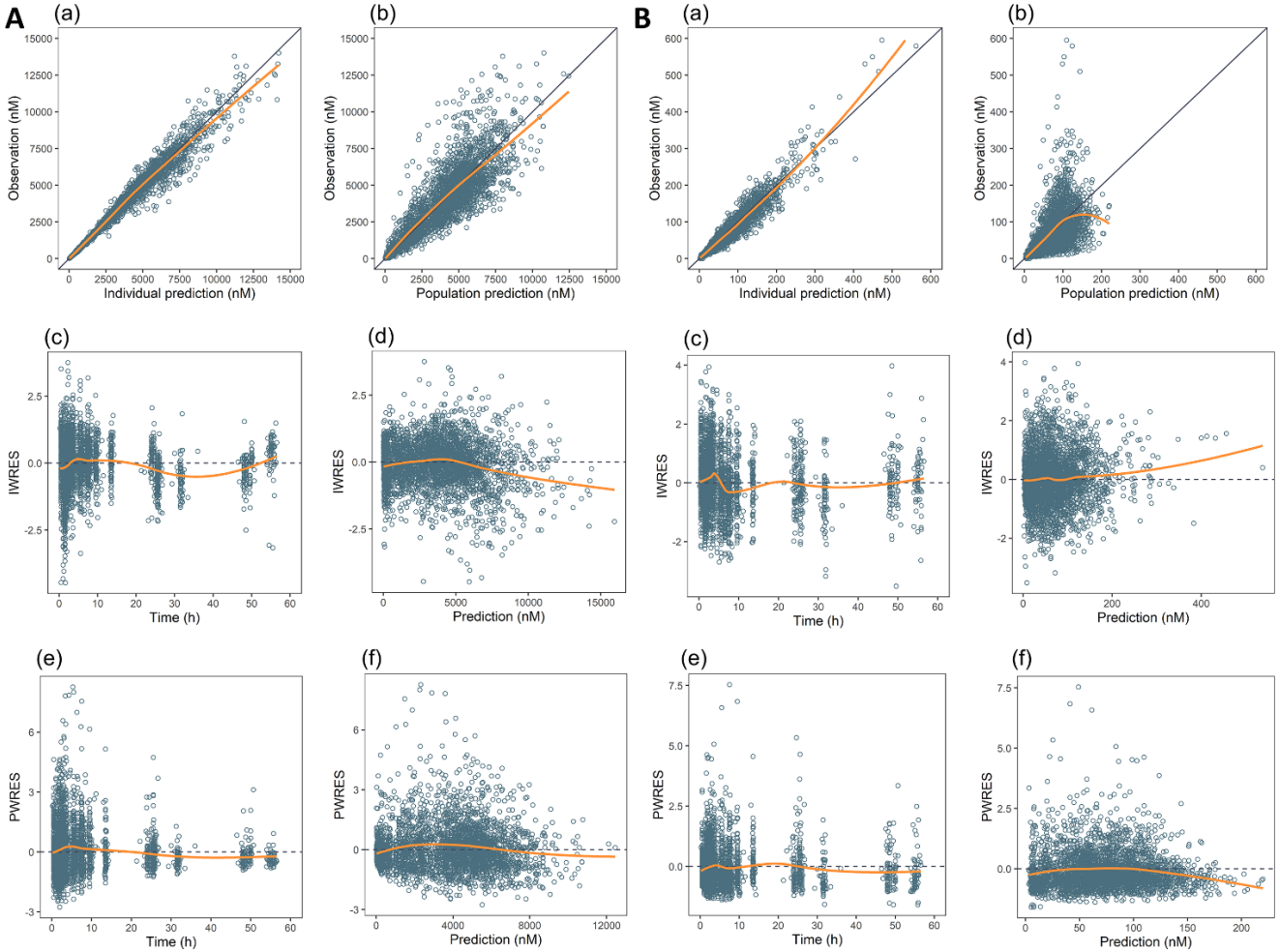

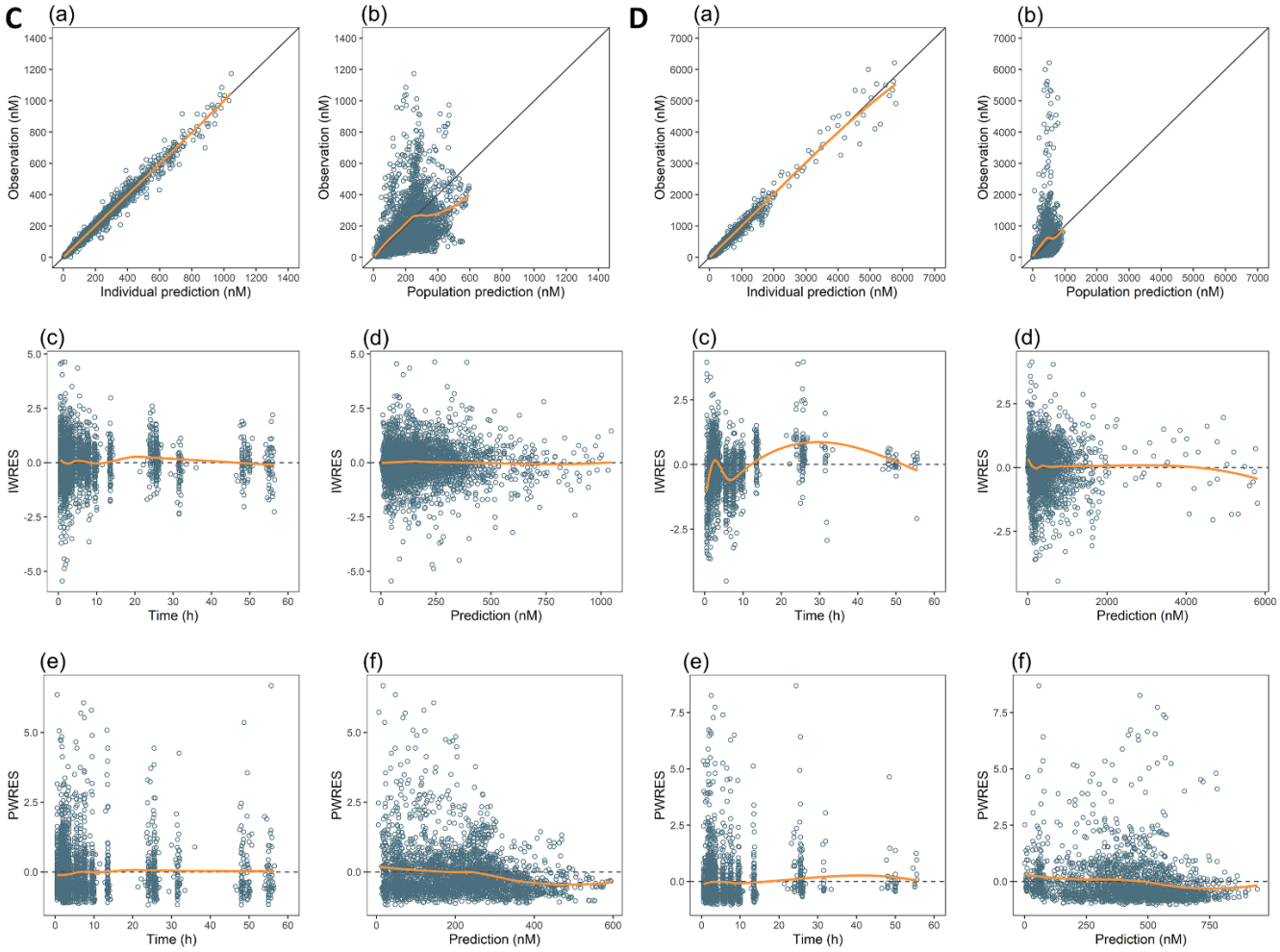
C
(a)
Observation (nM)
Individual prediction (nM)
(b)
Observation (nM)
Population prediction (nM)
(c)
IWRES
Time (h)
(d)
IWRES
Prediction (nM)
(e)
PWRES
Time (h)
(f)
PWRES
Prediction (nM)
D
(a)
Observation (nM)
Individual prediction (nM)
(b)
Observation (nM)
Population prediction (nM)
(c)
IWRES
Time (h)
(d)
IWRES
Prediction (nM)
(e)
PWRES
Time (h)
(f)
PWRES
Prediction (nM)

**Figure S5. Prediction-corrected visual predictive check (n=1,000) of the final model (Step 8 in Figure 1) of irinotecan (a), SN-38 (b), SN-38G (c), and APC (d).** The upper and lower blue shaded region denotes the 90% confidence intervals around the 10$^{th}$ and 90$^{th}$ percentiles of simulated concentrations, respectively. The pink shaded region denotes the 90% confidence intervals around the median (50$^{th}$ percentile) of simulated concentrations. The blue solid and black dashed lines represent the 10$^{th}$, median (50$^{th}$), and 90$^{th}$ percentiles of the observed and predicted plasma concentrations, respectively. The blue circles indicate the prediction-corrected observed plasma concentrations. The black circles indicate 10$^{th}$, median (50$^{th}$), and 90$^{th}$ percentiles of the predicted plasma concentrations.

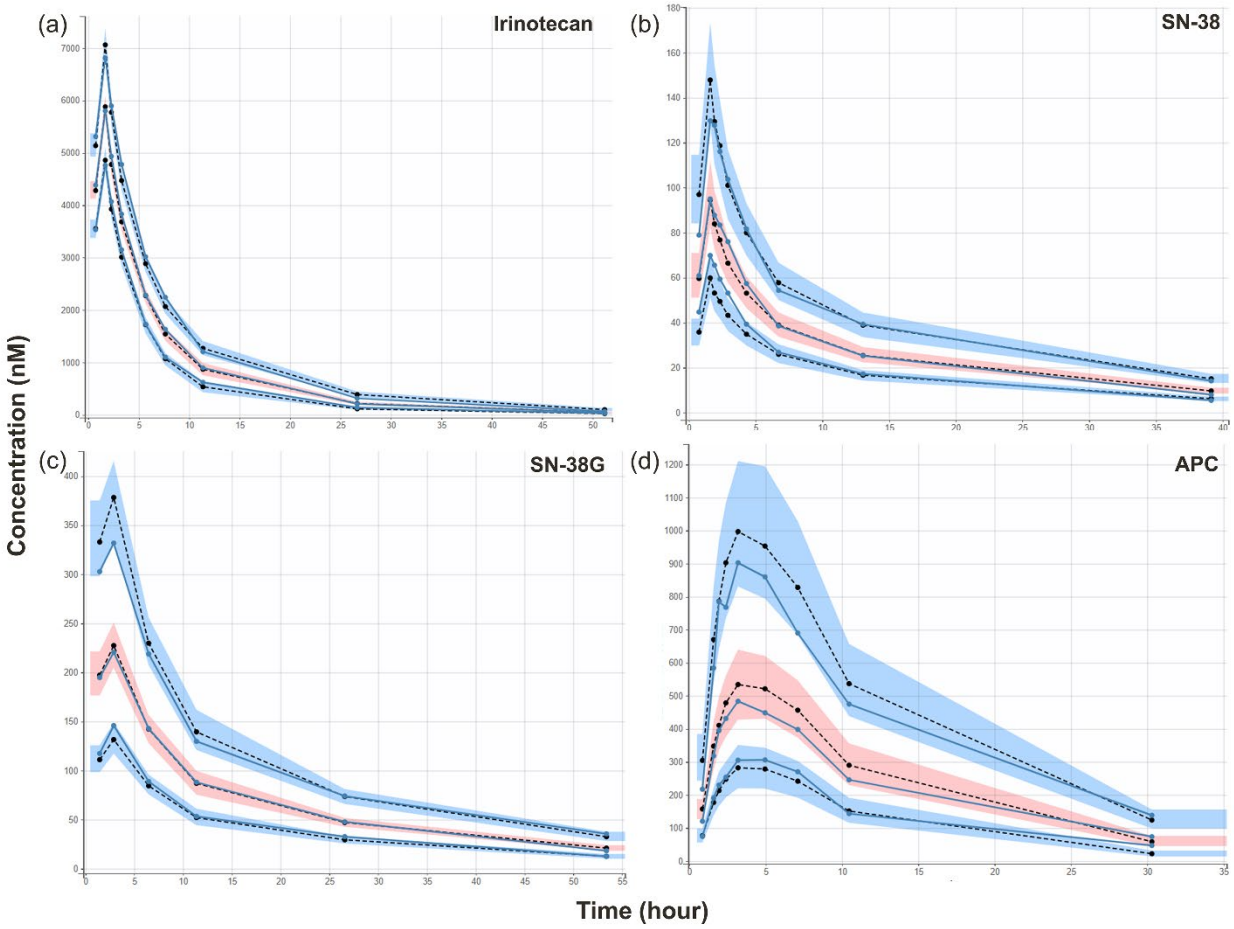

## 3. Supplementary Tables

**Table S1. 84 Very Important Pharmacogenes (VIPs) as classified by the PharmGKB database** (https://www.pharmgkb.org/) [7]. Genes in bold are involved in the disposition of irinotecan and SN-38 (https://www.pharmgkb.org/pathway/PA2001). Chr, chromosome.

| VIP | Chr | Position (GRCh37/hg19) | VIP | Chr | Position (GRCh37/hg19) |
|---|---|---|---|---|---|
| *ABCA1* | 9 | 107543283-107690527 | *HLA-DQB3* | 6 | 32698535-32699472 |
| ***ABCB1*** | **7** | **87133178-87342639** | *HMGCR* | 5 | 74632992-74657926 |
| *ABCB11* | 2 | 169779448-169887833 | *HSD11B2* | 16 | 67465035-67471454 |
| ***ABCC2*** | **10** | **101542354-101611949** | *HTR1A* | 5 | 63255874-63258119 |
| ***ABCG1*** | **21** | **43619798-43717354** | *HTR2A* | 13 | 47405676-47471211 |
| ***ABCG2*** | **4** | **89011415-89152474** | *KCNH2* | 7 | 150642043-150675402 |
| *ACE* | 17 | 61554421-61575741 | *LDLR* | 19 | 11200037-11244505 |
| *ADRB1* | 10 | 115803805-115806667 | *MAOA* | X | 43514154-43606071 |
| *ADRB2* | 5 | 148206155-148208197 | *NAT2* | 8 | 18248754-18258723 |
| *AHR* | 7 | 17338275-17385775 | *NPPB* | 1 | 11917520-11918992 |
| *ALOX5* | 10 | 45869623-45941567 | *NPR1* | 1 | 153651163-153666468 |
| *APOA1* | 11 | 116706468-116708338 | *NR3C1* | 5 | 142657495-142815077 |
| *ARID5B* | 10 | 63661012-63856707 | *NR3C2* | 4 | 148999914-149363672 |
| *BDNF* | 11 | 27676441-27743605 | *NTRK2* | 9 | 87283465-87638505 |
| *CACNA1C* | 12 | 2162415-2807115 | *PEAR1* | 1 | 156863522-156886226 |
| *CACNA1S* | 1 | 201008639-201081694 | *POR* | 7 | 75544419-75616173 |
| *CACNB2* | 10 | 18429605-18830688 | *PTGIS* | 20 | 48120410-48184707 |
| ***CES1*** | **16** | **55836763-55867075** | *PTGS1* | 9 | 125132808-125157982 |
| ***CES2*** | **16** | **66968346-66978994** | *RYR1* | 19 | 38924339-39078204 |
| *COMT* | 22 | 19929262-19957498 | *RYR2* | 1 | 237205701-237997288 |
| *CRHR1* | 17 | 43697709-43913194 | *SCN5A* | 3 | 38589552-38691164 |
| *CYP1A2* | 15 | 75041183-75048941 | *SLC15A2* | 3 | 121613170-121663034 |
| *CYP2A6* | 19 | 41349442-41356352 | *SLC22A1* | 6 | 160542862-160579750 |
| *CYP2B6* | 19 | 41497203-41524301 | *SLC22A2* | 6 | 160637793-160679963 |
| *CYP2C19* | 10 | 96522462-96612671 | *SLC22A3* | 6 | 160769404-160873611 |
| *CYP2C9* | 10 | 96698414-96749148 | *SLC22A6* | 11 | 62744068-62752495 |
| *CYP2D6* | 22 | 42522500-42526883 | *SLC47A1* | 17 | 19437166-19482346 |
| *CYP2R1* | 11 | 14899555-14913751 | *SLC47A2* | 17 | 19581627-19620043 |
| ***CYP3A4*** | **7** | **99354582-99381811** | *SLC6A3* | 5 | 1392904-1445543 |
| ***CYP3A5*** | **7** | **99245812-99277621** | *SLC6A4* | 17 | 28521336-28562986 |
| *DBH* | 9 | 136501484-136524466 | *SLCO1A2* | 12 | 21417533-21548371 |
| *DYPD* | 1 | 97543300-98386615 | ***SLCO1B1*** | **12** | **21284127-21392730** |
| *DRD1* | 5 | 174867674-174871163 | *SLCO1B3* | 12 | 20963637-21069843 |
| *DRD2* | 11 | 113280316-113346001 | *SLCO2B1* | 11 | 74862031-74917445 |
| *EGFR* | 7 | 55086724-55275031 | *TBXAS1* | 7 | 139478046-139720125 |
| *ESR1* | 6 | 152011630-152424408 | *TCL1A* | 14 | 96176303-96180533 |
| *FKBP5* | 6 | 35541361-35696360 | *TPMT* | 6 | 18128544-18155374 |
| *G6PD* | X | 153759604-153775801 | ***UGT1A1*** | **2** | **234668918-234681945** |
| *GLCCI1* | 7 | 8008373-8128709 | *UGT1A4* | 2 | 234627437-234681945 |

| | | | | | |
|---|---|---|---|---|---|
| *GRK4* | 4 | 2965342-3042474 | *VDR* | 12 | 48235319-48298814 |
| *GRK5* | 10 | 120967196-121215131 | *VKORC1* | 16 | 31102174-31106276 |
| *HLA-B* | 6 | 31321648-31324989 | *ZNF423* | 16 | 49524514-49891830 |

**Table S2. The number of measurements below the lower limit of quantification (LLOQ)**

| | | Concentration-time data | | | | |
|---|---|---|---|---|---|---|
| Compound | Trial | LLOQ (ng/mL) | ≥ LLOQ (n) | < LLOQ (n) | sum (n) | LLOQ (%) |
| CPT-11 | 1 | 10 | 10 | 1249 | 0 | 1249 |
| | 2 | 10 | 10 | 500 | 0 | 500 |
| | 3 | 10 | 10 | 1007 | 0 | 1007 |
| | 4 | 10 | 10 | 223 | 0 | 223 |
| | All trials | | 2979 | 0 | 2979 | 0 |
| SN-38 | 1 | 5 | 1165 | 0 | 1165 | 0 |
| | 2 | 5 | 490 | 0 | 490 | 0 |
| | 3 | 2 | 993 | 97 | 1090 | 8.90 |
| | 4 | 1 | 217 | 0 | 217 | 0 |
| | All trials | | 2865 | 97 | 2962 | 3.27 |
| SN-38G | 1 | 2.5 | 1248 | 1 | 1249 | 0.08 |
| | 2 | 2.5 | 498 | 0 | 498 | 0 |
| | 3 | 2.5 | 882 | 0 | 882 | 0 |
| | 4 | 1 | 223 | 0 | 223 | 0 |
| | All trials | | 2851 | 1 | 2852 | 0.04 |
| APC | 1 | 2.5 | 1163 | 0 | 1163 | 0 |
| | 2 | 2.5 | 477 | 0 | 477 | 0 |
| | 3 | 2.5 | 227 | 0 | 227 | 0 |
| | 4 | 1 | 223 | 0 | 223 | 0 |
| | All trials | | 2090 | 0 | 2090 | 0 |

**Table S3. Final pharmacokinetic parameter estimates and bootstrap results of irinotecan, SN-38, SN-38G, and APC (Step 8 of Figure 1).**

| | Final Model | | | Bootstrap Analysis (n=1000) | | |
|---|---|---|---|---|---|---|
| | **Mean** | **RSE(%)** | **Shrinkage (%)[f]** | **Median** | **95% CI** | **Difference (%)** |
| **Population mean (fixed effect)** | | | | | | |
| **Irinotecan** | | | | | | |
| CL1 (L/h) | 21.8 | 4.72 | - | 22.2 | 20.1 - 24.5 | -1.83 |
| COADM on CL1 | 0.375 | 20.7 | - | 0.377 | 0.214 - 0.530 | -0.533 |
| BSA on CL1 | 0.679 | 27.3 | - | 0.733 | 0.365 - 1.11 | -7.95 |
| rs4149057 in *SLCO1B1* on CL1 | 0.124 | 25.9 | - | 0.115 | 0.0468 - 0.182 | 7.26 |
| V1 (=V4) (L)[a] | 7.29 | 10.1 | - | 8.31 | 5.68 - 11.3 | -13.9 |
| CL12 (L/h) | 9.58 | 3.95 | - | 9.30 | 8.53 - 10.1 | 2.92 |
| V2 (L) | 108 | 3.93 | - | 113 | 104 - 123 | -4.63 |
| CL13 (L/h) | 383 | 4.16 | - | 372 | 337 - 416 | 2.87 |
| V3 (L) | 117 | 1.92 | - | 116 | 112 - 121 | 0.85 |
| a1 | 0.13 | 2.84 | - | 0.144 | 0.125 - 0.168 | -10.8 |
| a2 | 0.083 | 6.28 | - | 0.0876 | 0.0716 - 0.106 | -5.54 |
| $F_{m1}$(%)[b,c] | 10.5 | - | - | - | - | - |
| $F_{m2}$(%)[b,c] | 81.6 | - | - | - | - | - |
| $F_{m3}$(%)[b,c] | 7.62 | - | - | - | - | - |
| **SN-38** | | | | | | |
| CL4 (L/h) | 68.1 | 3.64 | - | 67.2 | 57.7 - 78.5 | 1.32 |
| Pre-treatment total bilirubin on CL4 | -0.298 | 21.1 | - | -0.312 | -0.515 - -0.0903 | -4.70 |
| rs887829 in *UGT1A1* on CL4 | -0.39 | 9.99 | - | -0.374 | -0.509 - -0.254 | 4.10 |
| *EGFR* rare variant burden on CL4 | -0.0896 | 32 | - | -0.0884 | -0.173 - -0.0139 | 1.34 |
| CL45 (L/h) | 27.2 | 8.15 | - | 29.9 | 16.4 - 45.5 | -9.93 |
| V5 (L) | 1.72E+04 | 12.3 | - | 17926 | 11935 - 31022 | -4.22 |
| $k_{tr}$ ($h^{-1}$) | 1.12 | 17.1 | - | 0.955 | 0.686 -1.57 | 14.7 |
| $k_a$ ($h^{-1}$) | 0.0466 | 4.88 | - | 0.0530 | 0.0435 - 0.0654 | -13.7 |
| F | 0.488 | 1.66 | - | 0.454 | 0.417 - 0.487 | 6.97 |
| $F_{m4}$ (%)[c] | 31 | 2.57 | - | 34.8 | 30.5 - 38.6 | -12.3 |
| **SN-38G** | | | | | | |
| CL6 (L/h) | 5.03 | 1.97 | - | 5.16 | 4.61 - 5.78 | -2.5 |
| V6 (L) | 3.64 | 2.91 | - | 3.67 | 3.25 - 4.14 | -0.82 |
| **APC** | | | | | | |
| CL7 (L/h) | 9.58 | 2.35 | - | 10.2 | 8.54 - 12.1 | -6.47 |
| V7 (L) | 30.3 | 2.78 | - | 32.2 | 26.9 - 38.4 | -6.27 |
| **Interindividual variability (%)** | | | | | | |

| | | | | | | |
|---|---|---|---|---|---|---|
| **Irinotecan** | | | | | | |
| CL1 | 33.7 | 4.87 | 0.0926 | 33.6 | 29.5 - 37.7 | 0.30 |
| V1 (=V4) | 144 | 8.02 | 0.843 | 148 | 105 - 208 | -2.70 |
| CL12 | 54.6 | 5.95 | -1.43 | 55.9 | 45.2 - 70.2 | -2.38 |
| V2 | 51.3 | 6.1 | -5.92 | 47.7 | 36.9 - 62.2 | 7.02 |
| CL13 | 56.6 | 6.73 | 2.25 | 53.5 | 43.2 - 64.8 | 5.48 |
| V3 | 27.3 | 5.24 | -5.39 | 26.8 | 23.7 - 30.0 | 1.83 |
| a1 | 38.7 | 5.68 | 7.29 | 43.2 | 33.7 - 52.8 | -11.6 |
| a2 | 96.0 | 5.84 | -0.846 | 93.8 | 75.7 - 113 | 2.29 |
| $F_{m1}$[d] | 24.7 | - | - | - | - | - |
| $F_{m2}$[d] | 9.14 | - | - | - | - | - |
| $F_{m3}$[d] | 73.5 | - | - | - | - | - |
| **SN-38** | | | | | | |
| CL4 | 32.0 | 5.69 | 9.32 | 29.2 | 17.2 - 41.8 | -2.10 |
| CL45 | 142 | 6.21 | -13.6 | 138 | 104 - 177 | 2.77 |
| $K_{tr}$ | 163 | 11.9 | 2.61 | 152 | 98.7 - 208 | 8.45 |
| $K_a$ | 46 | 8.52 | -7.18 | 44.3 | 25.9 - 64.4 | -0.68 |
| $F^e$ | 40.6 | 6.52 | 1.03 | 45.7 | 37.2 - 53.4 | -1.11 |
| $F_{m4}$[e] | 52.1 | 5.34 | 1.47 | 58.2 | 40.1 - 75.6 | 1.19 |
| **SN-38G** | | | | | | |
| CL6 | 24.1 | 6.61 | -8.82 | 24.7 | 15.3 - 32.3 | -2.49 |
| V6 | 33.7 | 6.52 | 0.853 | 32.4 | 21.9 - 41.8 | 3.86 |
| **APC** | | | | | | |
| CL7 | 26.0 | 6.8 | -11.8 | 27.1 | 15.1 - 37.1 | -4.23 |
| V7 | 31.9 | 7.2 | -5.66 | 30.9 | 21.9 - 41.8 | 3.13 |
| **Residual error** | | | | | | |
| **Irinotecan** | | | | | | |
| Additive error (nM) | 1.25 | 44.1 | - | 1.35 | 0.298 - 2.61 | -8.00 |
| Proportional error (%) | 0.099 | 1.71 | - | 0.10 | 0.0935 - 0.105 | -1.01 |
| **SN-38** | | | | | | |
| Additive error (nM) | 0.771 | 15 | - | 0.75 | 0.226 - 1.19 | 2.72 |
| Proportional error (%) | 0.191 | 2.21 | - | 0.19 | 0.178 - 0.210 | 0.52 |
| **SN-38G** | | | | | | |
| Additive error (nM) | 4.69 | 7 | - | 4.41 | 3.09 - 6.12 | 5.97 |
| Proportional error (%) | 0.0795 | 3.54 | - | 0.08 | 0.0652 - 0.0940 | -0.63 |
| **APC** | | | | | | |
| Additive error (nM) | 16.3 | 6.98 | - | 16.7 | 12.3 - 21.8 | -2.45 |
| Proportional error (%) | 0.105 | 4.12 | - | 0.104 | 0.0787 - 0.123 | 0.95 |

[a]During the structural model development, the identifiability issue was found in the volume of the central compartment of SN-38 (V4). Therefore, we addressed this issue by fixing V4 to the volume of the central compartment of irinotecan (V1).

[b]Secondary parameters (i.e. $F_{m1}$, $F_{m2}$, and $F_{m3}$) were calculated from the empirical Bayes post hoc estimates of a1 and a2 using the following equations: $F_{m1}$ = a1/(1+a1+a2), $F_{m2}$ = 1/(1+a1+a2), and $F_{m3}$ = a2/(1+a1+a2). The population mean of secondary parameters were presented as median.
[c]The median fractions metabolized were comparable to those from the mass-balance studies in cancer patients receiving irinotecan single agent or in combination [8,9].
[d]Coefficient of variation (%) for interindividual variability of the secondary parameter was calculated as 100×(standard deviation/mean).
[e]The parameters, F and $F_{m4}$, are assumed to be logit-normally distributed to constrain the parameter to be within a range of [0,1].
[f]The samples of the conditional distribution was used to avoid shrinkage [10]. Negative shrinkage indicates no shrinkage [11].

Abbreviations: **CL1**, clearance of irinotecan (CL1=(CL1·$F_{m1}$) + (CL1·$F_{m2}$) + (CL1·$F_{m3}$), where $F_{m1}$+$F_{m2}$+$F_{m3}$=1); **CL12**, slow inter-compartmental clearance of irinotecan; **CL13**, fast inter-compartmental clearance of irinotecan; **CL4**, clearance of SN-38 (CL4=(CL4·$F_{m4}$) + (CL4·(1-$F_{m4}$))); **CL45**, inter-compartmental clearance of SN-38; **CL6**, clearance of SN-38G; **CL7**, clearance of APC; **F**, fraction of irinotecan undergoing delayed metabolism to SN-38 through transit compartment process; **$F_{m1}$**, fraction of irinotecan dose metabolized to SN-38; **$F_{m2}$**, fraction of irinotecan dose eliminated through other routes; **$F_{m3}$**, fraction of irinotecan dose metabolized to APC; **$F_{m4}$**, fraction of SN-38 metabolized to SN-38G; **$k_{tr}$**, **$k_a$**, first-order transit rate constants; **$tr_1$**, **$tr_2$**, **$tr_3$**, transit compartments; **V1**, volume of the central compartment of irinotecan; **V2**, volume of the slow-equilibrating peripheral compartment of irinotecan; **V3**, volume of the fast-equilibrating peripheral compartment of irinotecan; **V4**, volume of the central compartment of SN-38; **V5**, volume of the peripheral compartment of SN-38; **V6**, volume of the central compartment of SN-38G; **V7**, volume of the central compartment of APC.

## References


1. Zheng, X., Levine, D., Shen, J., Gogarten, S. M., Laurie, C., and Weir, B. S., A high-performance computing toolset for relatedness and principal component analysis of SNP data., *Bioinformatics* **28**(24), 3326–3328 (2012).
2. Price, A. L., Patterson, N. J., Plenge, R. M., Weinblatt, M. E., Shadick, N. A., and Reich, D., Principal components analysis corrects for stratification in genome-wide association studies., *Nat. Genet.* **38**(8), 904–909 (2006).
3. Akaike, H., A new look at the statistical model identification, *IEEE Trans. Automat. Contr.* **19**(6), 716–723 (1974).
4. Schwarz, G., Estimating the Dimension of a Model, *Ann. Stat.* **6**(2), 461–464 (1978).
5. Hothorn, T., Hornik, K., and Zeileis, A., Unbiased Recursive Partitioning: A Conditional Inference Framework, *J. Comput. Graph. Stat.* **15**(3), 651–674 (2006).
6. Strasser, H. and Weber, C., On the Asymptotic Theory of Permutation Statistics, *Math. Methods Stat. 8*(8), 220–250 (1999).
7. Gordon, A. S., Fulton, R. S., Qin, X., Mardis, E. R., Nickerson, D. A., and Scherer, S., PGRNseq: a targeted capture sequencing panel for pharmacogenetic research and implementation., *Pharmacogenet. Genomics* **26**(4), 161–168 (2016).
8. Slatter, J. G., Schaaf, L. J., Sams, J. P., Feenstra, K. L., Johnson, M. G., Bombardt, P. A., et al., Pharmacokinetics, metabolism, and excretion of irinotecan (CPT-11) following I.V. infusion of [(14)C]CPT-11 in cancer patients, *Drug Metab. Dispos.* **28**(4), 423–433 (2000).
9. Sparreboom, A., de Jonge, M. J., de Bruijn, P., Brouwer, E., Nooter, K., Loos, W. J., et al., Irinotecan (CPT-11) metabolism and disposition in cancer patients, *Clin. Cancer Res.* **4**(11), 2747–2754 (1998).
10. Lavielle, M. and Ribba, B., Enhanced Method for Diagnosing Pharmacometric Models: Random Sampling from Conditional Distributions, *Pharm. Res.* **33**(12), 2979–2988 (2016).
11. Lixoft, Understanding shrinkage and how to circumvent it (accessed 5 March 2021).